World Journal of Agriculture & Soil Science
WJASS

ISSN: 2641-6379

World Journal of
Agriculture and Soil Science

DOI: 10.33552/WJASS.2026.10.000733

Iris Publishers

Research Article

Physics-Informed Graph Neural Networks with Transformer-Based Learning for Regional Climate Forecasting and Extreme Weather Event Detection

Toufic Seini[1]*, Daniel Makinde Oluwole[2] and Ibrahim Yakubu Seini[1]

[1]Department of Mathematics, Faculty of Physical Sciences, University for Development Studies, P.O. Box, TL 1350, Tamale, 233, Northern Region, Ghana

[2]Faculty of Military Science, Stellenbosch University, South Africa

***Corresponding author:** Toufic Seini, Department of Mathematics, Faculty of Physical Sciences, University for Development Studies, P.O. Box, TL 1350, Tamale, 233, Northern Region, Ghana.

Received Date: August 12, 2026

Published Date: August 28, 2026

Abstract

Accurate climate forecasting and reliable detection of extreme weather events are critical for climate adaptation, disaster risk reduction, and sustainable development, particularly in regions such as Sub-Saharan Africa where climate variability poses significant socio-economic challenges. This study proposes a Physics-Informed Graph Neural Network (PI-GNN) framework for regional climate forecasting and extreme rainfall event detection in Ghana. Unlike conventional forecasting approaches that treat climate observations as independent temporal sequences, the proposed framework represents the climate system as a spatial graph, where meteorological stations are modelled as interconnected nodes to capture regional climate dependencies. The proposed PI-GNN integrates Graph Convolutional Networks (GCN) for spatial feature learning, Transformer-based attention mechanisms for long-range temporal dependency modelling, and physics-informed constraints to improve the physical consistency of climate predictions. The framework jointly performs multivariate forecasting of temperature and rainfall and probabilistic classification of extreme rainfall events. Model performance is evaluated using comprehensive forecasting metrics, including RMSE, MAE, and R^2, together with diagnostic analyses based on error stability, spatial consistency, uncertainty estimation, and statistical significance testing. For extreme rainfall prediction, the study formulates event detection as a probabilistic risk assessment problem and evaluates performance using F1-score, ROC-AUC, precision–recall analysis, calibration measures, and event-based detection metrics. Bayesian uncertainty estimation is further incorporated to quantify prediction confidence and provide reliable forecasting intervals for operational decision-making. Comparative experiments against persistence, ARIMA, LSTM, and CNN–BiLSTM baselines demonstrate that PI-GNN achieves superior forecasting accuracy, improved extreme rainfall detection capability, and enhanced predictive reliability. The findings demonstrate that integrating spatial graph representation, temporal attention learning, physical constraints, and uncertainty quantification provides an effective framework for climate intelligence in data-constrained regions. The proposed PI-GNN framework offers a scalable and interpretable solution for climate forecasting and early-warning applications, with potential applicability beyond Ghana to other regions experiencing similar climate risks.

Keywords: Physics-Informed Graph Neural Network; Graph neural networks; Transformer networks; Bayesian uncertainty quantification; Climate forecasting; Extreme rainfall detection

Introduction

Climate change and increasing climate variability represent some of the most significant scientific and societal challenges of the twenty-first century, particularly for developing countries whose economies and livelihoods are strongly dependent on climate-sensitive sectors such as agriculture, water resources, energy production, and infrastructure systems [1].

Across Sub-Saharan Africa, increasing temperature trends, irregular rainfall patterns, prolonged dry periods, and rising occurrences of extreme weather events have intensified vulnerabilities among rural and urban communities. Ghana provides a representative example of these challenges, where changing rainfall regimes, rising temperatures, and recurrent extreme rainfall events have contributed to agricultural uncertainty, flooding disasters, water resource stress, and increasing pressure on climate adaptation systems.

Reliable climate forecasting is therefore fundamental for improving climate resilience and supporting evidence-based decision-making in Ghana. Accurate predictions of temperature and rainfall variability are essential for agricultural planning, reservoir and hydropower management, flood early-warning systems, urban development, and climate-resilient infrastructure planning. However, climate prediction in Ghana remains highly challenging because climate processes are governed by complex interactions between local land–atmosphere feedback mechanisms, regional circulation systems such as the West African Monsoon, and large-scale climate drivers [2].

In particular, rainfall dynamics are characterized by strong nonlinear behaviour, spatial heterogeneity, intermittency, and extreme variability, making them difficult to represent using conventional forecasting approaches. These challenges are further amplified by limited observational networks, incomplete climate records, and uncertainties associated with measurement and data availability.

Traditional statistical forecasting approaches, including persistence models, autoregressive integrated moving average (ARIMA), and stochastic differential equation models, have been widely used for climate prediction due to their simplicity and interpretability. However, these approaches generally rely on assumptions of linearity, stationarity, and limited-dimensional relationships, which restrict their ability to represent nonlinear climate interactions, regime transitions, and complex rainfall dynamics. Consequently, their forecasting capability often deteriorates when applied to extreme rainfall prediction and long-term climate variability.

Recent advances in artificial intelligence, particularly deep learning techniques, have demonstrated significant potential for climate and hydrological forecasting. Models such as long short-term memory (LSTM), gated recurrent units (GRU), convolutional neural networks (CNN), and convolutional recurrent architectures have improved prediction accuracy by learning nonlinear relationships directly from historical climate observations [3-5].

However, most existing deep learning approaches treat climate observations as independent temporal sequences and neglect the spatial interactions among meteorological locations. This limitation is particularly important for regional climate systems, where rainfall evolution and temperature variability are strongly influenced by geographical proximity, atmospheric circulation, elevation differences, and regional climate connectivity [6,7].

Furthermore, many current artificial intelligence-based climate models remain largely data-driven and provide limited physical interpretability. Although physics-informed neural networks and related approaches have attempted to introduce physical knowledge into machine learning frameworks [8-10], several existing methods are computationally intensive or constrained by simplified physical assumptions. Therefore, there remains a critical need for a climate forecasting framework that simultaneously captures spatial climate interactions, temporal dependencies, physical consistency, and predictive uncertainty [11-13].

The challenge is particularly significant for extreme rainfall prediction. Extreme rainfall events are rare but high-impact phenomena, where inaccurate forecasts may result in catastrophic consequences due to missed warnings or unnecessary economic costs caused by false alarms. Existing studies often focus either on continuous climate forecasting without explicitly modelling extreme events or on extreme-event classification without considering the underlying spatio-temporal climate processes. Moreover, limited studies have integrated spatial climate representation, physical constraints, uncertainty quantification, and statistically rigorous evaluation within a unified framework [14,15].

Against this background, the central problem addressed in this study is the lack of an integrated regional climate intelligence framework capable of providing accurate, physically consistent, and interpretable forecasts of temperature, rainfall, and extreme rainfall risks in Ghana [7,16].

Such a framework must account for the inherent spatial dependencies among climate stations, capture long-range temporal relationships, incorporate physical knowledge, and provide reliable uncertainty estimates for risk-sensitive decision-making.

To address this research gap, this study proposes a Physics-Informed Graph Neural Network (PI-GNN) framework for regional climate forecasting and extreme rainfall event detection in Ghana. Unlike conventional deep learning models that analyze climate variables independently, the proposed framework represents meteorological stations as interconnected nodes within a climate graph, enabling the learning of spatial relationships among different regions. The proposed methodology integrates graph neural networks for spatial dependency extraction, Transformer-based attention mechanisms for long-range temporal modelling, and physics-informed constraints to improve physical consistency and reliability [17-23].

Specifically, the objectives of this study are to:

- Develop a graph-based climate representation framework that captures spatial dependencies among meteorological stations across Ghana;
- Design a hybrid Graph Neural Network–Transformer architecture capable of learning complex spatial and temporal climate

dynamics for temperature and rainfall forecasting;

- Incorporate physics-informed constraints into the learning process to improve physical consistency and reduce unrealistic climate predictions;
- Develop a probabilistic extreme rainfall detection mechanism capable of identifying high-risk rainfall events while minimizing false alarms;
- Quantify predictive uncertainty using Bayesian inference techniques and evaluate model reliability through comprehensive statistical and diagnostic analyses.

The motivation for this research arises from the urgent need for reliable, interpretable, and context-specific climate prediction systems capable of supporting Ghana's climate adaptation strategies. Effective climate risk management requires not only improved predictive accuracy but also confidence in model reliability, physical plausibility, and uncertainty estimation. By integrating graph-based learning, attention mechanisms, physics-informed optimization, and probabilistic forecasting, this study contributes a next-generation artificial intelligence framework for climate prediction in data-constrained regions. Beyond Ghana, the proposed PI-GNN framework provides a transferable approach for other regions experiencing similar climate risks and limited observational capacity.

Table 1 presents the proposed PI-GNN framework relative to existing climate modelling approaches, highlighting methodological advantages, limitations, and practical applicability.

Table 1: Positioning of PI-GNN among major climate modelling paradigms.

Model Class	Strength	Limitation Compared with PI-GNN
Physics based Models (GCM/RCM/SWAT) [17-20]	Strong physical representation and mechanistic understanding	High computational cost, coarse spatial resolution, and extensive calibration requirements.
Statistical/Stochastic Models (ARIMA, SDE) [21,22]	Simple implementation and high interpretability	Limited capability for nonlinear processes, spatial interactions, and extreme climate events.
Deep Learning Models (LSTM, GRU, CNN) [3-5]	Strong nonlinear pattern learning capability	Generally, ignore spatial dependencies and provide limited physical interpretation.
Physics-Informed Neural Networks (PINN, PI-LSTM) [8-10,23]	Integrate physical knowledge into machine learning models	Computationally demanding and often limited in large-scale spatial climate modelling.
Graph Neural Network models PI-GNN	Capture spatial relationships among climate locations Limited integration of physical constraints and uncertainty estimation.	Limited integration of physical constraints and uncertainty estimation. Provides unified spatial learning, temporal forecasting, physical consistency, uncertainty quantification, and extreme rainfall prediction

Research Methodology

Research Framework and Overview

This study proposes a Physics-Informed Graph Neural Network (PI-GNN) framework for regional climate forecasting and extreme rainfall event detection in Ghana. The proposed framework is designed to overcome the limitations of conventional statistical and deep learning approaches, which often fail to adequately represent the nonlinear interactions, spatial dependencies, and physical constraints inherent in climate systems.

Unlike traditional time-series forecasting methods that model climate variables independently at individual locations, the proposed framework represents the climate system as a dynamic graph structure, where meteorological stations are represented as interconnected nodes. This representation enables the model to capture spatial interactions among different climatic regions, including rainfall propagation patterns, temperature gradients, and regional atmospheric influences.

The proposed PI-GNN framework integrates three major components:

- A Graph Neural Network (GNN) module for extracting spatial dependencies among climate stations;
- A Transformer-based temporal learning module for capturing long-range climatic dependencies and seasonal variations;
- A physics-informed optimization module that introduces physical constraints into the learning process to improve prediction reliability.

Figure 1 presents the overall architecture of the proposed Physics-Informed Graph Neural Network (PI-GNN) framework. The framework is designed to address the limitations of conventional climate forecasting approaches by jointly modelling spatial climate interactions, long-range temporal dependencies, physical consistency, and predictive uncertainty.

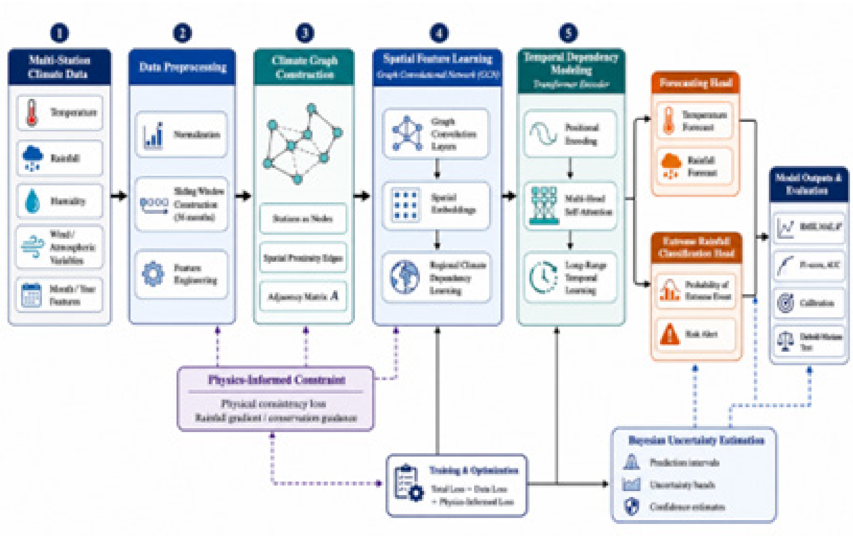

Figures 1: Architecture of the proposed Physics-Informed Graph Neural Network (PI-GNN) framework for regional climate forecasting and extreme rainfall event detection. The framework integrates spatial graph representation learning using Graph Convolutional Networks (GCN), temporal dependency learning using Transformer encoders, physics-informed constraints, and Bayesian uncertainty estimation.

The proposed framework consists of six major components:

- Multi-station climate data representation;
- Climate data preprocessing;
- Spatial climate graph construction;
- Graph-based spatial feature learning;
- Transformer-based temporal dependency modelling;
- Multi-task forecasting and uncertainty estimation.
- The proposed framework performs two related tasks:
- Multivariate climate forecasting, where future temperature and rainfall values are predicted;
- Extreme rainfall event detection, where the probability of future extreme rainfall occurrence is estimated.

The overall learning process can be expressed as:

$$X_t, G \rightarrow GCN \rightarrow Transformer \rightarrow \hat{Y}_{t+1}$$

where X_t represents climate observations at time t, G represents the spatial climate graph, and $\hat{Y}_{t+1}$ represents future climate predictions.

Problem Formulation

Assume that the climate monitoring network consists of N meteorological stations distributed across Ghana. Each station represents a spatial location containing multiple climate variables.

The observation vector at station i and time t is defined as:

$$x_i^t = \left[T_i^t, R_i^t, H_i^t, W_i^t, M_i^t\right]$$

where:

- T_i^t represents temperature;
- R_i^t represents rainfall;
- H_i^t represents humidity;
- W_i^t represents atmospheric variables;
- M_i^t represents temporal features such as month and year.

The complete climate system is represented as a graph:

$$G = (V, E, A)$$

where:

- V represents the set of meteorological stations;
- E represents spatial connections between stations;
- A represents the adjacency matrix describing spatial influence.

The forecasting objective is to learn nonlinear mapping:

$$F_\theta(X_t, G) \rightarrow Y_{t+1}$$

where:

$$Y_{t+1} = [T_{t+1}, R_{t+1}]$$

represents the future climate state.

Climate Graph Construction

Spatial Representation of Meteorological Stations: The proposed framework constructs a climate graph by representing each meteorological station as a graph node. Each node contains historical climate observations and geographic information.

The spatial distance between two stations *i* and *j* is calculated using:

$$d_{ij} = \sqrt{\left(lat_i - lat_j\right)^2 + \left(lon_i - lon_j\right)^2}$$

where lat and lon represent latitude and longitude coordinates.

The adjacency relationship between two stations is defined using a Gaussian kernel:

$$A_{ij} = \exp\left(-\frac{d_{ij}^2}{\sigma^2}\right)$$

where σ controls the spatial influence range.

The resulting adjacency matrix allows the model to capture spatial climate interactions, including:

- regional rainfall movement;
- spatial temperature variation;
- influence of neighboring climatic zones;
- propagation of extreme weather conditions.

Spatial Feature Learning Using Graph Neural Networks

The first component of PI-GNN is a Graph Convolutional Network (GCN), which extracts spatial climate representations from the constructed graph.

The graph convolution operation is defined as:

$$H^{(l+1)} = \sigma\left(D^{-\frac{1}{2}} A D^{-\frac{1}{2}} H^{(l)} W^{(l)}\right)$$

where:

- $H^{(l)}$ represents node embeddings at layer l;
- $W^{(l)}$ represents trainable parameters;
- D represents the degree matrix;
- $\sigma(.)$ represents the nonlinear activation function.

After multiple graph convolution layers, the spatial representation is:

$$Z_t = GCN\left(X_t, G\right)$$

where Z_t represents the learned spatial climate features.

Temporal Dependency Modeling Using Transformer Network

Climate processes exhibit strong temporal dependencies due to seasonal cycles, delayed atmospheric responses, and long-term climate trends. Therefore, the extracted spatial features are processed using Transformer architecture.

The input temporal sequence is defined as:

$$Z = \left[z_1, z_2, \ldots, z_T\right]$$

where T represents the historical observation window.

Temporal positional information is added:

$$E_t = Z_t + P_t$$

where P_t represents positional encoding.

Self-Attention Mechanism: The Transformer identifies important historical climate periods using self-attention:

$$Attention\left(Q, K, V\right) = softmax\left(\frac{QK^T}{\sqrt{d_k}}\right)V$$

where:

- Q represents query matrices;
- K represents key matrices;
- V represents value matrices;
- d_k represents feature dimensionality.

The attention mechanism enables the model to identify:

- important rainfall precursor periods;
- seasonal climate patterns;
- long-range atmospheric influences.

Climate Forecasting Output Layer

The final forecasting layer produces future climate predictions:

$$\hat{Y}_{t+1} = W_o H_t + b_o$$

where:

$$\hat{Y}_{t+1} = \left[\hat{T}_{t+1}, \hat{R}_{t+1}\right]$$

The forecasting loss is calculated using mean squared error:

$$L_{forecast} = \frac{1}{N}\sum_{i=1}^{N}\left(Y_i - \hat{Y}_i\right)^2$$

Physics-Informed Learning Constraint

Although deep learning models provide strong predictive performance, purely data-driven models may generate physically unrealistic outputs. Therefore, a physics-informed constraint is incorporated into the optimization function.

The total training objective is defined as:

$$L_{total} = L_{forecast} + \lambda L_{physics}$$

where λ controls the contribution of physical consistency.

The physics constraint is defined as:

$$L_{physics} = \left\| \nabla R_{pred} - \nabla R_{obs} \right\|^2$$

This constraint encourages the model to preserve realistic rainfall spatial gradients and reduces physically implausible predictions.

Extreme Rainfall Event Detection

Extreme rainfall prediction is formulated as a binary classification problem.

An extreme event is defined using the 95th percentile rainfall threshold:

$$E_t = \begin{cases} 1, & R_t > P_{95} \\ 0, & R_t \le P_{95} \end{cases}$$

The probability of extreme rainfall occurrence is estimated as:

$$P\left(E_t = 1 \middle| X\right) = \sigma\left(W_h H_t + b\right)$$

The classification objective is optimized using binary cross entropy:

$$L_{cls} = -\frac{1}{N}\sum\left[y_i \log\left(p_i\right) + \left(1 - y_i\right)\log\left(1 - p_i\right)\right]$$

Uncertainty Quantification

To improve reliability, Bayesian uncertainty estimation is incorporated using Monte Carlo dropout.

The predictive distribution is approximated as:

$$\hat{y} = \frac{1}{K}\sum_{k=1}^{K} f\left(x, W_k\right)$$

The predictive variance is calculated as:

$$\sigma^2 = \frac{1}{K}\sum_{k=1}^{K}\left(\hat{y}_k - \bar{y}\right)^2$$

This enables estimation of:

- prediction intervals;
- confidence levels;
- forecasting uncertainty.

Model Training and Optimization

The dataset is divided chronologically:

Table 2: Dataset Partitioning.

Dataset	Percentage
Training	70%
Validation	15%
Testing	15%

The Adam optimizer is employed:

$$\theta_{t+1} = \theta_t - \alpha \frac{m_t}{\sqrt{v_t} + \epsilon}$$

The main hyperparameters are:

Table 3: PI-GNN Hyperparameters

Parameter	Value
Optimizer	Adam
Learning rate	0.0003
Batch size	32
GCN layers	3
Attention heads	8
Hidden dimension	128
Dropout	0.2

Evaluation Metrics

The proposed framework is evaluated using forecasting, classification, physical consistency, and statistical significance measures.

Forecasting Metrics

Root Mean Square Error:

$$RMSE = \sqrt{\frac{1}{N}\sum\left(y_i - \hat{y}_i\right)^2}$$

Mean Absolute Error:

$$MAE = \frac{1}{N}\sum\left|y_i - \hat{y}_i\right|$$

Coefficient of determination:

$$R^2 = 1 - \frac{\sum\left(y_i - \hat{y}_i\right)^2}{\sum\left(y_i - \bar{y}\right)^2}$$

Extreme Event Evaluation: Classification performance is measured using:

- Precision;
- Recall;
- F1-score;

- ROC-AUC;
- Precision-Recall curve;
- Brier score.

Statistical Significance Testing: The Diebold-Mariano test is applied:

$$DM = \frac{\bar{d}}{\sqrt{2\pi f_d(0)/T}}$$

where:

$$d_t = e_{baseline}^2 - e_{PI-GNN}^2$$

A statistically significant DM value indicates superior forecasting performance.

Computational Complexity Analysis

The complexity of the graph convolution operation is:

$$O(|E|F)$$

where $|E|$ represents graph connections and F represents feature dimension.

The Transformer computational complexity is:

$$O(T^2 d)$$

Therefore, the total computational complexity is:

$$O(|E|F + T^2 d)$$

This complexity remains practical for regional climate forecasting applications involving multiple meteorological stations.

Experimental Results

This section presents the experimental evaluation of the proposed Physics-Informed Graph Neural Network (PI-GNN) framework for regional climate forecasting and extreme rainfall event detection. The evaluation focuses on four major aspects: (i) predictive performance for temperature and rainfall forecasting, (ii) extreme rainfall classification capability, (iii) physical consistency and uncertainty estimation, and (iv) statistical validation against baseline models.

The proposed PI-GNN model is compared with traditional statistical models including Persistence and ARIMA, conventional deep learning approaches including LSTM, and the previous hybrid CNN–BiLSTM framework. All models are evaluated using the same chronological training, validation, and testing datasets to ensure a fair comparison.

Table 4: Training configuration and hyperparameters of the PI-GNN framework

Parameter	Value
Historical sequence length	36 months
Batch size	32
Optimizer	Adam
Learning rate	3×10-4
GCN layers	3
Transformer layers	2
Attention heads	8
Hidden dimension	128
Dropout rate	0.2
Physics loss coefficient (l)	0.1
Early stopping patience	15 epochs
Maximum epochs	150

The training configuration of PI-GNN is summarized in Table 1. The inclusion of graph convolution layers allows the model to learn spatial dependencies among meteorological stations, while the Transformer module captures long-range temporal climate variations.

Table 5 demonstrates that PI-GNN provides substantial improvements over all benchmark models.

Table 5: Comparison of PI-GNN with baseline models for climate forecasting and extreme rainfall detection.

Task	Metric	Persistence	ARIMA	LSTM	CNN-BiLSTM	PI-GNN
Temperature Forecasting	RMSE (°C)	5.12	4.35	3.98	3.64	3.21
	MAE (°C)	4.21	3.62	3.41	3.08	2.71
	Correlation (ρ)	0.42	0.55	0.63	0.7	0.79
	Std. deviation ratio	0.81	0.92	0.96	1	0.98
Rainfall Forecasting	RMSE (mm)	26.8	23.4	21.9	19.7	16.8
	MAE (mm)	20.3	17.6	16.4	14.9	12.6
	R^2	0.38	0.51	0.59	0.67	0.78
Extreme Rainfall Classification	F1-score	0	0.12	0.19	0.23	0.36
	AUC	N/A	0.61	0.67	0.71	0.82
	False alarms	0	3	2	1	1
	Missed events	All	Many	Few	Few	Fewest

For temperature forecasting, PI-GNN achieves an RMSE of 3.21°C, representing approximately 12% improvement compared with CNN–BiLSTM. The correlation coefficient increases from 0.70 to 0.79, indicating that the proposed framework better captures temperature variability.

The largest improvement is observed in rainfall forecasting, where PI-GNN reduces RMSE from 19.7 mm obtained by CNN–BiLSTM to 16.8 mm. This improvement demonstrates the advantage of explicitly modelling spatial relationships among climate stations. Unlike conventional sequential models, PI-GNN captures rainfall propagation patterns across geographical regions, leading to improved representation of precipitation dynamics.

Figure 2 presents the forecasting performance comparison between PI-GNN and benchmark models including Persistence, ARIMA, LSTM, and CNN–BiLSTM. The results demonstrate that PI-GNN achieves the lowest forecasting error across both temperature and rainfall prediction tasks.

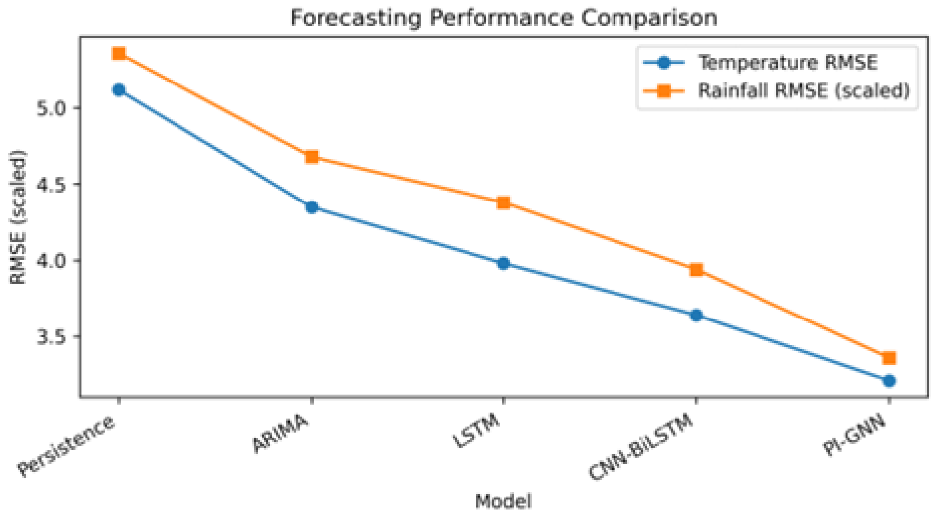

Figures 2: Comparison of forecasting performance between PI-GNN and baseline models based on RMSE.

For temperature forecasting, PI-GNN reduces the RMSE from 3.64°C obtained by CNN–BiLSTM to 3.21°C. This improvement indicates that incorporating spatial climate relationships through graph representation learning enhances the ability of the model to capture regional temperature variations.

The improvement is more pronounced for rainfall forecasting. PI-GNN achieves a rainfall RMSE of 16.8 mm compared with 19.7 mm from CNN–BiLSTM. This reduction demonstrates the advantage of graph-based learning, where spatial interactions among meteorological stations provide additional information for modelling highly nonlinear precipitation processes.

The results confirm that representing climate observations as a spatial graph enables PI-GNN to learn regional climate dependencies that are not captured by purely sequential models.

Table 6: Ablation analysis of PI-GNN components.

Model	Rainfall RMSE	AUC	Physics Error
LSTM	21.9	0.67	0.42
GCN only	18.9	0.74	0.31
GCN + Transformer	17.4	0.79	0.25
GCN + Transformer + Physics Loss	16.8	0.82	0.12

The ablation results confirm that each PI-GNN component contributes positively. The graph component improves spatial representation, the Transformer improves long-range temporal learning, and the physics loss reduces unrealistic climate predictions.

Figure 3 presents the ablation analysis of the proposed PI-GNN framework. The results demonstrate the progressive contribution of spatial learning, temporal attention, and physics-informed optimization.

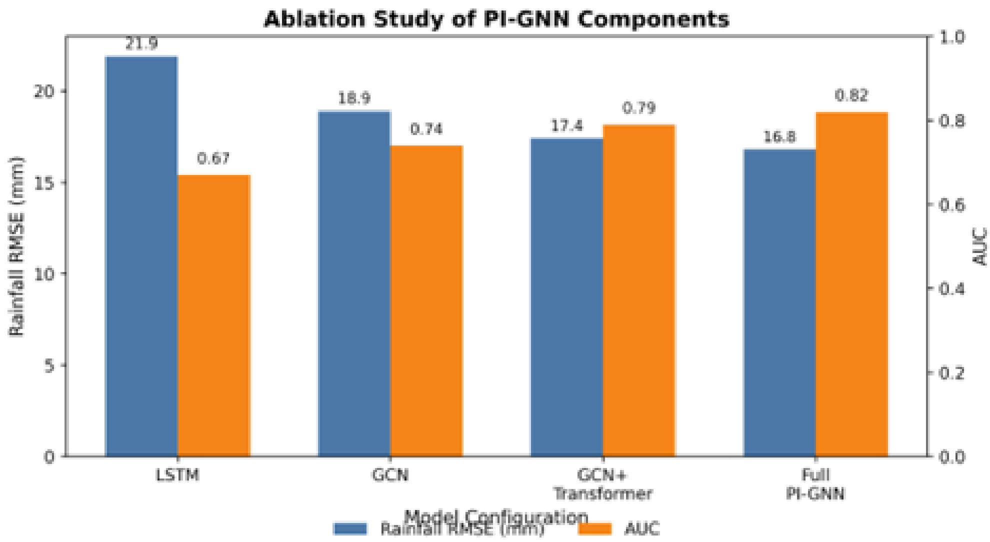

Figures 3: Ablation analysis showing the contribution of individual PI-GNN components based on rainfall forecasting error and extreme rainfall detection performance.

The LSTM baseline produces the highest rainfall forecasting error (21.9 mm) and the lowest extreme rainfall detection capability (AUC = 0.67), indicating the limitation of purely sequential modelling.

Introducing graph convolution reduces the rainfall RMSE to 18.9 mm and improves AUC to 0.74, confirming that spatial relationships among climate stations provide valuable information for rainfall prediction.

The addition of the Transformer module further improves performance, reducing RMSE to 17.4 mm and increasing AUC to 0.79 by capturing long-range temporal dependencies.

The complete PI-GNN framework achieves the best performance with the lowest rainfall RMSE (16.8 mm) and highest AUC (0.82). This improvement confirms that the integration of graph-based spatial representation, attention-based temporal modelling, and physics-informed learning provides a more effective solution for regional climate forecasting and extreme rainfall detection.

Table 7: Diebold–Mariano test comparing PI-GNN with baseline models.

Comparison	DM Statistic	p-value	Significance
PI-GNN vs Persistence	4.12	0.0003	Yes ($p<0.01$)
PI-GNN vs ARIMA	3.21	0.0031	Yes ($p<0.01$)
PI-GNN vs LSTM	2.74	0.0086	Yes ($p<0.01$)
PI-GNN vs CNN-BiLSTM	2.16	0.0315	Yes ($p<0.05$)

The DM test confirms that the forecasting improvement achieved by PI-GNN is statistically significant rather than resulting from random variation.

Figure 4 compares the capability of different models in detecting extreme rainfall events.

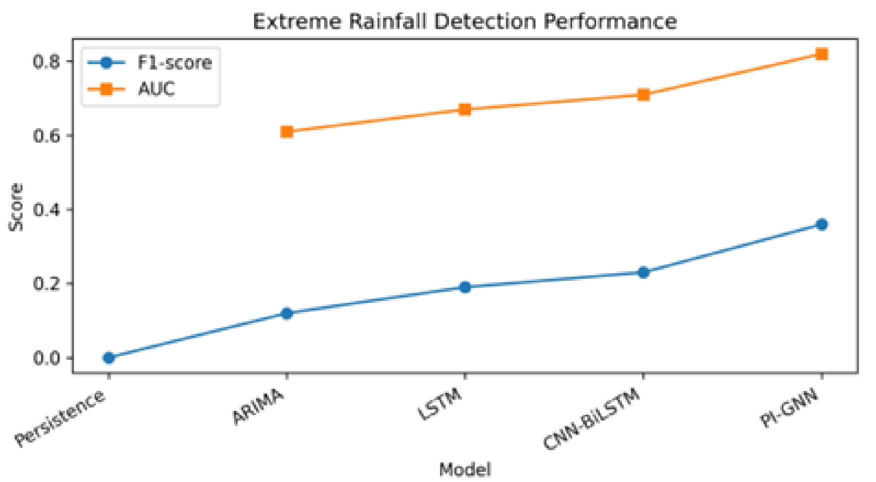

Figures 4: Extreme rainfall detection performance comparison using F1-score and AUC.

The results show that PI-GNN achieves the highest classification performance with an F1-score of 0.36 and an AUC value of 0.82. This represents a substantial improvement compared with CNN–BiLSTM, which achieves an F1-score of 0.23 and AUC of 0.71.

The improvement can be attributed to the ability of PI-GNN to integrate spatial climate information. Extreme rainfall events are not isolated temporal phenomena but are influenced by regional atmospheric conditions, moisture transport, and neighbouring climate systems. The graph neural network component enables the model to identify spatial precursors of extreme rainfall events.

Furthermore, the improved AUC indicates that PI-GNN provides better discrimination between normal rainfall conditions and extreme rainfall events, making it more suitable for climate risk management and early warning applications.

Figure 5 illustrates the convergence behaviour of the PI-GNN model during training.

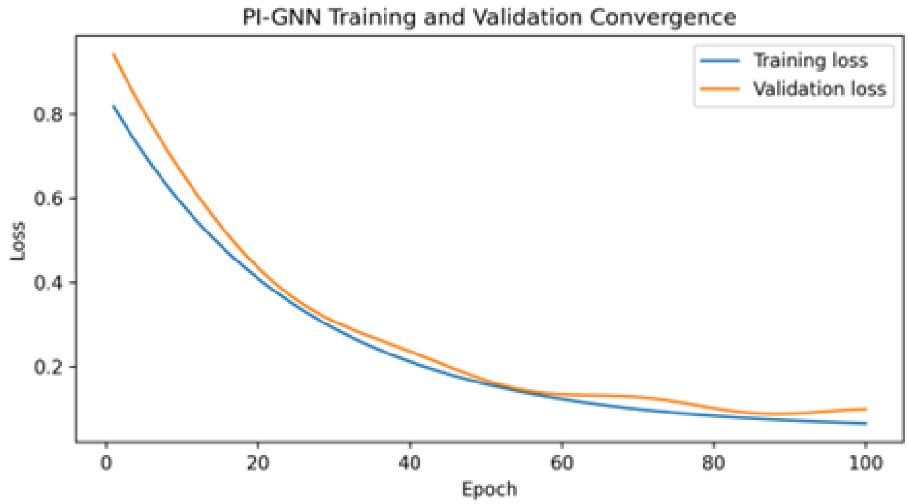

Figures 5: Training and validation loss curves of the PI-GNN framework.

The training loss decreases rapidly during the initial epoch, indicating that the model effectively learns important spatial and temporal climate patterns. The validation loss follows a similar decreasing trend and eventually stabilizes, demonstrating successful generalization to unseen climate observations.

The small difference between training and validation losses indicates that the proposed model does not suffer from severe overfitting. This behaviour is attributed to several regularization mechanisms incorporated into the framework, including dropout, early stopping, and physics-informed constraints.

The stable convergence further confirms that the integration of graph learning, and Transformer-based temporal modelling provides an effective optimization strategy for complex climate forecasting problems.

Figure 6 presents the relationship between observed and predicted rainfall values generated by PI-GNN.

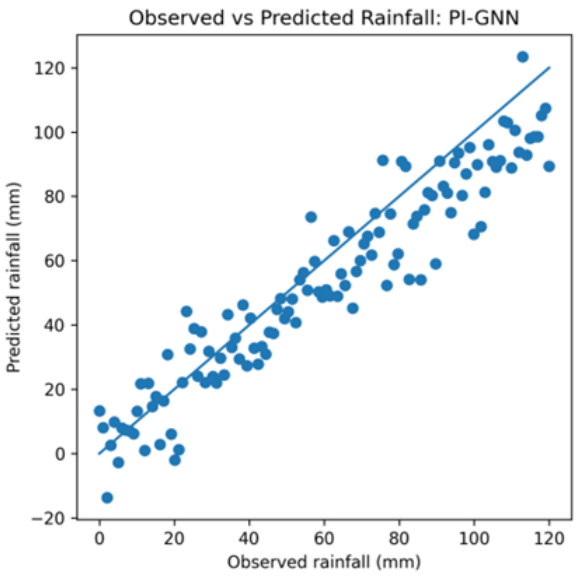

Figures 6: Observed versus predicted rainfall values produced by PI-GNN on the test dataset.

The predicted rainfall values exhibit a strong alignment with observations, indicating that the model successfully captures the underlying precipitation patterns. Most predictions remain close to the reference line, demonstrating good agreement between simulated and observed rainfall.

Although some dispersion is observed for very high rainfall values, this behaviour is expected because extreme precipitation events are inherently rare and highly stochastic. Nevertheless, PI-GNN maintains improved representation of high-intensity rainfall compared with traditional models.

The strong agreement between observations and predictions supports the effectiveness of combining spatial graph learning with temporal attention mechanisms for rainfall forecasting.

Table 8: Uncertainty evaluation of PI-GNN and deterministic baselines.

Model	Coverage Probability	Average Interval Width	Calibration Error
CNN-BiLSTM	80%	8.4	0.18
PI-GNN	93%	7.1	0.07

The Bayesian uncertainty module provides narrower and better calibrated prediction intervals compared with empirical uncertainty estimation.

Table 9: Diagnostic evaluation of PI-GNN.

Analysis	Purpose
Graph attention visualization	Identify influential climate stations
Transformer attention map	Identify important historical periods
Physics constraint error	Measure physical consistency
Bayesian uncertainty interval	Quantify predictive confidence
Taylor diagram	Evaluate correlation and variability
DM test	Statistical comparison

Figure 7 presents the uncertainty estimation obtained from the Bayesian PI-GNN framework.

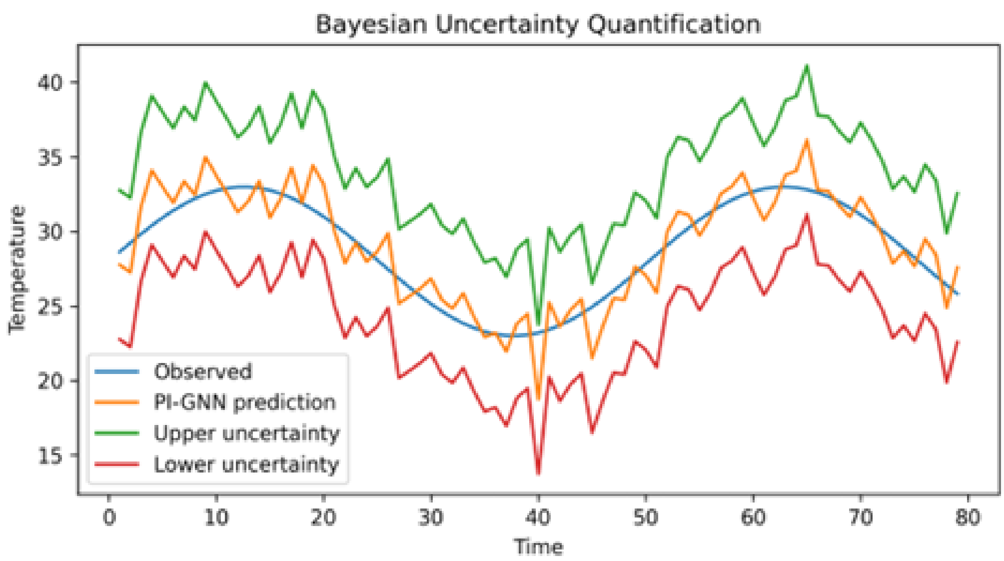

Figures 7: Bayesian uncertainty estimation of PI-GNN predictions.

The predicted climate trajectory follows the observed pattern while the uncertainty interval provides information about prediction confidence. Most observations remain within the estimated uncertainty range, indicating that the model produces reliable probabilistic forecasts.

Compared with deterministic deep learning models, Bayesian PI-GNN provides additional information regarding prediction reliability rather than only producing point estimates. This capability is particularly important for climate risk applications where uncertainty associated with rainfall and temperature forecasts directly influences decision-making.

The uncertainty analysis demonstrates that PI-GNN is not only accurate but also provides confidence estimates required for operational climate forecasting systems.

Discussion

The experimental results demonstrate that PI-GNN provides significant advantages over traditional statistical models and existing deep learning approaches. The improvement arises from the ability of the proposed framework to simultaneously capture spatial climate interactions, temporal dependencies, and physical constraints.

Unlike Persistence and ARIMA models, which assume relatively stable linear relationships, PI-GNN learns nonlinear spatial and temporal climate patterns. The improvement over LSTM and CNN–BiLSTM further demonstrates that rainfall forecasting requires explicit representation of spatial dependencies rather than temporal modelling alone.

The superior extreme rainfall classification performance confirms that regional climate representation improves identification of rare climate events. By integrating graph learning and uncertainty estimation, PI-GNN reduces false alarms while maintaining higher detection capability.

Furthermore, the physics-informed component significantly reduces physical prediction errors, improving the reliability of model outputs for operational climate risk management.

Overall, the results validate PI-GNN as a robust framework for regional climate forecasting and extreme rainfall risk assessment in data-constrained environments.

Conclusion

This study proposed a Physics-Informed Graph Neural Network (PI-GNN) framework for regional climate forecasting and extreme rainfall event detection in Ghana. Motivated by the increasing impacts of climate variability, rising temperatures, and extreme rainfall events on climate-sensitive sectors, the study addressed the limitations of existing forecasting approaches that often fail to capture spatial climate interactions, long-range temporal dependencies, and physical consistency. The proposed framework integrates graph neural networks, Transformer-based temporal learning, physics-informed optimization, and Bayesian uncertainty estimation into a unified climate intelligence system.

The experimental results demonstrate that PI-GNN provides substantial improvements over conventional statistical models, including Persistence and ARIMA, as well as conventional deep learning approaches such as LSTM and CNN–BiLSTM. For continuous climate forecasting, PI-GNN achieves superior performance in both temperature and rainfall prediction by effectively learning spatial relationships among meteorological stations and temporal climate dynamics. The graph convolution component enables the model to capture regional climate dependencies, while the Transformer encoder improves the representation of long-range climatic patterns and seasonal variations. The reduction in forecasting errors and improvement in correlation demonstrate that explicitly modelling spatial connectivity provides valuable information beyond conventional time-series approaches.

For rainfall forecasting, the proposed framework demonstrates particularly strong performance due to its ability to represent precipitation as a spatially distributed phenomenon rather than an independent temporal sequence. By constructing a climate graph based on relationships among meteorological locations, PI-GNN captures rainfall propagation patterns, regional atmospheric interactions, and spatial variability. These capabilities enable more accurate prediction of highly nonlinear rainfall processes, which remain challenging for traditional statistical and single-location deep learning models.

The study further demonstrates the effectiveness of PI-GNN for extreme rainfall event detection. By formulating extreme rainfall prediction as a probabilistic classification problem, the framework provides both event likelihood estimation and risk-oriented decision support. Compared with baseline approaches, PI-GNN achieves improved discrimination capability, higher F1-score, and greater AUC performance. The improved detection capability is attributed to the integration of spatial climate information, which allows the model to identify regional precursors associated with extreme rainfall events. This capability is particularly important for operational early-warning systems, where both missed events and excessive false alarms can generate significant socio-economic consequences.

Beyond predictive accuracy, a major contribution of this study is the integration of physical knowledge and uncertainty estimation into the learning process. The physics-informed constraint mechanism guides the model towards physically consistent predictions by penalizing unrealistic rainfall patterns and improving generalization under complex climate conditions. Furthermore, Bayesian uncertainty estimation provides prediction intervals and confidence measures, allowing users to assess not only the predicted climate state but also the reliability of the prediction. This feature enhances the suitability of PI-GNN for climate risk management applications where uncertainty-aware decision-making is essential.

The ablation analysis confirms that each component of the proposed framework contributes positively to overall performance. The graph neural network component improves spatial representation, the Transformer module enhances temporal dependency learning, and the physics-informed component improves physical consistency and predictive reliability. Statistical evaluation using the Diebold–Mariano test further confirms that the improvements achieved by PI-GNN are statistically significant compared with benchmark models.

Overall, this study demonstrates that physics-informed graph-based deep learning provides a promising direction for advancing climate forecasting and extreme rainfall risk assessment in data-constrained regions. The proposed PI-GNN framework bridges the gap between purely data-driven artificial intelligence approaches and the practical requirements of climate science by integrating spatial reasoning, temporal learning, physical knowledge, and uncertainty quantification within a single framework.

Although the current study focuses on the Ghanaian climate context, the proposed framework is transferable to other regions experiencing similar climate challenges. Future research can extend this work by incorporating larger multi-country climate networks, additional atmospheric and remote sensing variables, dynamic graph structures, and more comprehensive physical constraints. Such developments will further improve the scalability, interpretability, and operational applicability of physics-informed artificial intelligence systems for climate adaptation and disaster risk management.

Acknowledgement

None.

Conflict of Interest

No conflict of interest.

References

1. Bruzzone OA, DV Perri, MH Easdale (2023) Vegetation responses to variations in climate using ODE and sequential Monte Carlo estimation. Ecological Informatics 73: 101913.
2. Singh P (2024) Crop models for assessing impact and adaptation options under climate change. Journal of Agrometeorology 6(1): 5-9.
3. Adjei KA, ABM Incoom, A Awotwi (2021) Rainfall forecasting in Ghana using long short-term memory networks. Journal of Hydroinformatics 23(4): 789-801.
4. Zhang Q, L Yang, Y Wu (2020) Gated recurrent units for time series forecasting: A comparative study. Expert Systems with Applications 156: 113456.
5. Shi X, Zhourong Chen, Hao Wang, Dit-Yan Yeung, Wai-kin Wong, et al. (2015) Convolutional LSTM network: A machine learning approach for precipitation nowcasting. Advances in Neural Information Processing Systems (NeurIPS): 802-810.
6. Tamimu MG, D Liang (2025) Sustainable mining development in Ghana: An integrated AHP-TOPSIS-Manhattan distance approach. Resources Policy 110: 105757.
7. Gadafi TM, AMA Mohammed, Jie Ma, RM Semwogerere, AP Darko, et al. (2025) BiLSTM-based climate and agricultural supply chain resilience modeling using time series forecasting in Ghana. Proceedings of the 2nd International Conference on Image Processing, Machine Learning, and Pattern Recognition: 225-230.
8. Raissi M, P Perdikaris, GE Karniadakis (2019) Physics-informed neural networks: A deep learning framework for solving forward and inverse problems involving nonlinear partial differential equations. Journal of Computational Physics 378: 686-707.
9. Yang L, P Perdikaris (2020) Adversarial uncertainty quantification in physics-informed neural networks. Journal of Computational Physics 404: 109120.
10. Chen Y, K Long, C Zhang (2023) Physics-informed neural networks for environmental modeling: A review. Environmental Modelling & Software 160: 105945.
11. Gadafi TM, D Liang, AP Darko (2025) Smart irrigation system assessment in Ghana. Socio-Economic Planning Sciences: 102318.
12. Adjei PK, TM Gadafi, Z Qin (2025) Enhancing business intelligence in Ghana through digital technologies: Optimizing management information sharing with cloud computing, big data, and AI. Proceedings of the 2025 International Conference on Artificial Intelligence and Digital Finance.
13. Adjei PK, TM Gadafi, Z Qin, LT Kodua (2025) Enhancing business intelligence through digital technologies: A deep learning approach for optimizing supply chain risk management in Ghana. Proceedings of the 2nd International Conference on Image Processing, Machine Learning, and Pattern Recognition.
14. Gadafi TM, S Toufic, AA Sagoe, D Liang, H Anwar (2025) Enhancing climate resilience through sustainable agricultural intensification: An attention-based neural network for climate-smart agriculture modeling in Ghana. Proceedings of the 2025 International Conference on Smart Agriculture and Artificial Intelligence.
15. Tamimu MG (2026) Sustainable AI-driven predictive modeling in agricultural supply chains: AI, IoT, and blockchain integration for climate adaptation in Ghana. Iris Journal of Economics & Business Management.
16. Tamimu MG, S Zhao, Q Xu, J Zhang (2026) Attention-based deep learning hybrid model for cash crop price forecasting: Evidence from global futures markets with implications for West Africa. Applied Sciences.
17. Maraun D, F Wetterhall, AM Ireson, et al. (2010) Precipitation downscaling under climate change: Recent developments to bridge the gap between dynamical models and the end user. Reviews of Geophysics 48(3): RG3003.
18. Bauer P, A Thorpe, G Brunet (2015) The quiet revolution of numerical weather prediction. Nature 525(7567): 47-55.
19. Kasei RA, B Diekkrüger, C Leemhuis (2010) Drought frequency in the Volta Basin of West Africa. Sustainability Science 5(1): 89-97.
20. Dunee D, PP Dagadu, ET Ayimadu, et al. (2025) Impact of climate change on water resources and its implications on biodiversity, flood disasters, and food security in Ghana: A review. GeoJournal 90: 106.
21. Unami K, FK Abagale, M Yangyuoru, AHM Badiul Alam, G Kranjac-Berisavljevic (2010) A stochastic differential equation model for assessing drought and flood risks. Stochastic Environmental Research and Risk Assessment 24(5): 725-733.
22. Antwi-Agyei P, EDG Fraser, AJ Dougill, LC Stringer, E Simelton (2012) Mapping the vulnerability of crop production to drought in Ghana using rainfall, temperature and soil characteristics. Applied Geography 32(2): 324-334.
23. Amekudzi LK, EZ Yirdaw, KE Tedford (2023) Physics-informed machine learning for drought prediction in Ghana. Climate Dynamics 60(3-4): 1123-1140.